Exploring the evolution of giant molecular clouds in one of the nearest spiral galaxies M33

Ayu Konishi[1], **Kazuyuki Muraoka[1]**, **Kazuki Tokuda[2,3]**,
Shinji Fujita[4], **Rin I. Yamada[5]**, **Fumika Demachi[5]**, **Kengo Tachihara[5]**,
Yasuo Fukui[5], **Masato I. N. Kobayashi[3]**, **Tsuge Kisetsu[6]**,
Akiko Kawamura[3] and **Toshikazu Onishi[1]**

[1]Department of Physics, Graduate School of Science, Osaka Metropolitan University, 1-1 Gakuen-cho, Naka-ku, Sakai, Osaka 599-8531, Japan

[2]Department of Earth and Planetary Sciences, Faculty of Sciences, Kyushu University, Nishi-ku, Fukuoka 819-0395, Japan

[3]National Astronomical Observatory of Japan, National Institutes of Natural Sciences, 2-21-1 Osawa, Mitaka, Tokyo 181-8588, Japan

[4]Institute of Astronomy, the University of Tokyo, 2-21-1 Osawa, Mitaka, Tokyo 181-0015, Japan

[5]Department of Physics, Nagoya University, Chikusa-ku, Nagoya 464-8602, Japan

[6]Dr. Karl Remeis Observatory and ECAP, Universität Erlangen-Nürnberg, Sternwartstraße 7, 96049, Bamberg, Germany

Abstract. The evolution of giant molecular clouds (GMCs), which are the main sites of star formation, is essential for unraveling how stars form and how galaxies evolve. We analyzed the M33 CO($J = 2$–1) data with spatial resolution of 39 pc obtained by ALMA-ACA 7 m array combined with IRAM 30 m. We identified 736 GMCs and classified them into three types; Type I: associated with no H ii regions, Type II: associated with H ii regions with the Hα luminosity $L(H\alpha) < 10^{37.5}$erg s^{-1}, Type III: associated with H ii regions with $L(H\alpha) > 10^{37.5}$erg s^{-1}. We found that mass, size, and velocity dispersion of GMCs slightly increase in the order of Type I, II, and III GMCs. Type III GMCs mainly exist in the spiral arm, while many of Type I and Type II GMCs are distributed in the inter-arm. Assuming that the star formation proceeds steadily, we roughly estimated the total GMC lifetime of 30 Myr.

Keywords. ISM: molecules, stars: formation, galaxies: spiral, galaxies: Local Group

1. Introduction

Giant molecular clouds (GMCs) are the primary reservoirs of cold, dense molecular gas and the birthplace of stars in galaxies. Massive stars can cause supernova explosions, release and supply heavy elements to interstellar space, and have a profound effect on the evolution of galaxies. Large-scale molecular gas survey toward the Large Magellanic Cloud (LMC) by the NANTEN 4 m telescope found that the GMCs are classified into three types according to activities of massive star formation: Type I shows no signature of massive star formation; Type II is associated with only H ii region(s); and Type III with both H ii region(s) and young stellar cluster(s) (YSCs) (Fukui et al. 1999; Kawamura et al. 2009). They argued that these types indicate the evolutionary sequence of GMCs. Such studies of

the GMC type classification were extended to the nearest spiral galaxy M33, which is one of the best targets to study the GMC evolution because of its proximity ($D \sim 840$ kpc, Freedman et al. 2001) and the moderate inclination angle ($i \sim 55°$, Koch et al. 2018). The CO all-disk survey of M33 by IRAM 30 m telescope detected over five hundred GMCs (Gratier et al. 2012; Druard et al. 2014). Corbelli et al. (2017) compared the GMCs with multi-wavelength data set and classified the GMCs into different evolutionary stages. More recently, Similar studies on star-formation and the GMCs evolution have been advanced toward the nearby spiral galaxies thanks to the Physics at High Angular Resolution in Nearby GalaxieS (PHANGS) ALMA survey (e.g., Schinnerer et al. 2019; Pan et al. 2022). In this study, we reexamine the GMC evolution in M33 based on the higher spatial (~ 39 pc) and higher velocity (~ 0.7 km s^{-1}) resolution CO($J = 2$–1) data by the 7 m antennae of the Atacama Compact Array (ACA).

2. Large-scale CO($J = 2$–1) survey in M33 by the ACA 7 m array

The ^{12}CO, ^{13}CO, C^{18}O ($J = 2$–1) observation toward M33 was performed with the ACA stand-alone mode (project code 2018.A.00058.S; PI: K. Muraoka, 2017.1.00901.S and 2019.1.01182.S; PI: E. Rosolowsky). ALMA data reduction was carried out using the Common Astronomy Software Application (CASA) package (McMullin et al. 2007) version 5.4.0 and the `tclean` task implemented in the CASA package (Cornwell 2008) with input parameters; weighting = natural, deconvolver = `multi-scale`, usemask = `auto-multithresh`. The final synthesized beam is 7.″31 × 6.″50 (30 pc × 26 pc), and its position angle is −28.92 deg for ^{12}CO data with a grid size of 1.″5. The ACA survey setting and data analyses in detail were described in (Muraoka et al. 2022).

We combined the ACA 7 m array and IRAM 30 m ^{12}CO data with the `feathering` task. We spatially smoothed the ^{12}CO data to be ~ 39 pc in order to compare our data with the GMC-type classification in LMC reported by Kawamura et al. (2009) at the same resolution. Our ^{12}CO data sensitivity is ~ 0.02–0.04 K at a velocity resolution of 0.7 km s^{-1}.
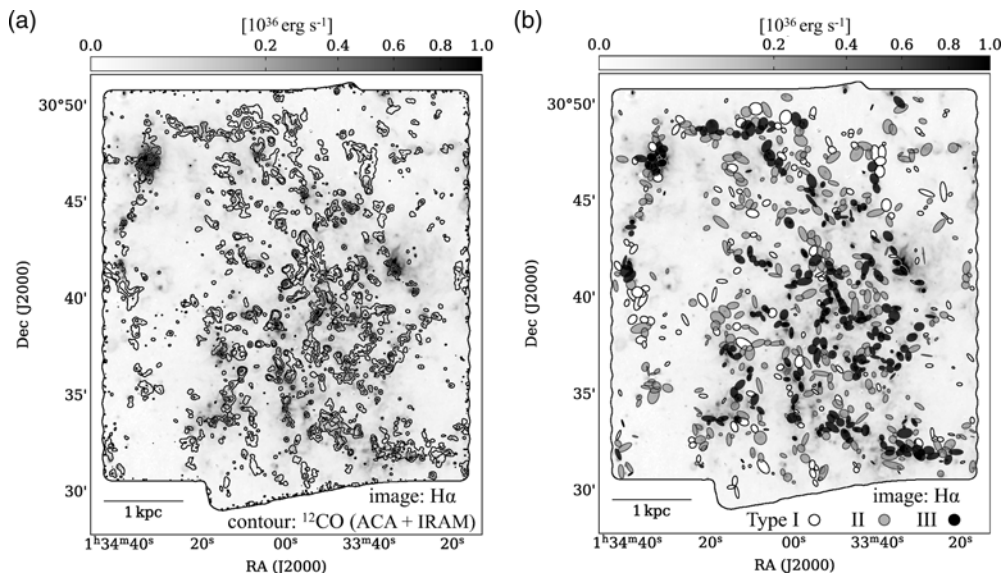
3. Results & Discussion

3.1. *Identification of GMCs*

Figure 1 (a) shows the ^{12}CO($J = 2$–1) emission from M33 obtained by the ACA 7 m array + IRAM 30 m with a spatial resolution of ~ 39 pc. We applied cloud identification algorithm `PYCPROPS` to the ^{12}CO cube data. We briefly describe this algorithm and identification procedure because the details are described in Rosolowsky et al. (2021). `PYCPROPS` first extracts all "local maxima" of input cube data and then removes some of them which are considered noise with threshold parameters. We set the local maxima to be more than 3σ (`delta` parameter) and a number of cube pixels of them (`min_pix` parameter) corresponds to twice the beam size of the ^{12}CO($J = 2$–1) data. `PYCPROPS` extrapolated parameters of identified structures such as second moment of the major (σ_{maj}) and minor (σ_{min}) axes, velocity dispersion, and integrated intensity in order to remove sensitivity bias when we measure physical properties of clouds. We deconvolved a radius R of each cloud by the beam size σ_{beam} of ~ 39 pc as follows:

$$R = 1.91\sqrt{(\sigma_{\mathrm{maj}}^2 - \sigma_{\mathrm{beam}}^2)^{0.5}(\sigma_{\mathrm{min}}^2 - \sigma_{\mathrm{beam}}^2)^{0.5}}. \tag{3.1}$$

Finally, we obtained 736 GMCs with masses between $10^{3.6}\,M_\odot$ and $10^{6.5}\,M_\odot$ using a CO-to-H$_2$ conversion factor $X_{\mathrm{CO}} = 4.0 \times 10^{20}$ cm^{-2} / (K km s^{-1}) and CO($J = 2$–1) / CO($J = 1$–0) ratio $R_{21} = 0.6$ (Muraoka et al. 2022).

Figure 1. (a) ^{12}CO($J = 2$–1) emission from M33 obtained by the ACA 7 m array + IRAM 30 m with a spatial resolution of $\sim$39 pc. Gray scale shows the Hα image by KPNO 2.1 m (Hoopes & Walterbos 2000; Hoopes et al. 2001) which cut to fit the ACA observation field. ^{12}CO contour levels are 0.15, 0.5, 2 K, respectively. (b) Distribution of GMCs in each type on Hα image. White, gray, and black ellipses represent Type I, II, and III GMCs, respectively.

3.2. *Classification of GMCs based on the Hα luminosity*

There are large variations in star formation activity between GMCs; e.g., the association with star clusters and/or H II regions. In LMC, Yamaguchi et al. (2001) found that Hα luminosity, $L(\text{H}\alpha)$, of the H II regions associated with GMCs increases as GMCs evolve. The frequency distributions of Hα luminosity are offset between Type II GMCs which is associated with only H II regions and Type III GMCs which is associated with both H II regions and YSCs, and overlapping at $L(\text{H}\alpha)$ of $\sim 10^{37.5}$erg s^{-1}.

In this study, we try classifying GMCs into following the three types based on the association with H II regions and Hα luminosities;

Type I   :   GMCs associated with no H II regions (inactive massive star-forming region)
Type II   :   GMCs associated with H II regions with $L(\text{H}\alpha) < 10^{37.5}$erg s^{-1}
Type III :   GMCs associated with H II regions with $L(\text{H}\alpha) > 10^{37.5}$erg s^{-1}

We defined the association of GMCs and H II regions if the spatial extent of a GMC is overlapped with the Hα emitting region identified by `astrodendro` (Rosolowsky et al. 2008) which is suitable for finding hierarchical structures such as H II regions and diffuse ionized gas. We set three `astrodendro` parameters; `min_value`: the minimum intensity value is 2.0×10^{34} erg s^{-1}, `min_delta`: the minimum height to be "leaf" is 1.0×10^{34} erg s^{-1} which corresponds to about 5 sigma, `min_npix`: the minimum number of two-dimensional pixels in the RA, Dec axes is 25 (1 pix = 1.5"). `astrodendro` eventually identified 769 H II regions as leaves. This type classification yields 182 Type I GMCs, 316 Type II GMCs, and 238 Type III GMCs. Table 1 summarize the classification results and Figure 1 (b) shows the distribution of GMCs in each type on Hα image.

Table 1. GMC type and their physical properties.

| GMC Type	Type I	Type II	Type III
Number	182 (25 %)	316 (43 %)	238 (32 %)
Mass ($M_\odot$)	$\sim 7.1 \times 10^4$	$\sim 1.6 \times 10^5$	$\sim 3.2 \times 10^5$
Radius (pc)	~ 34	~ 44	~ 50
Velocity dispersion (km s^{-1})	~ 2.43	~ 3.03	~ 3.37
Timescale (Myr)	7	13	10

Notes: The median of mass, radius, and velocity dispersion of GMCs.
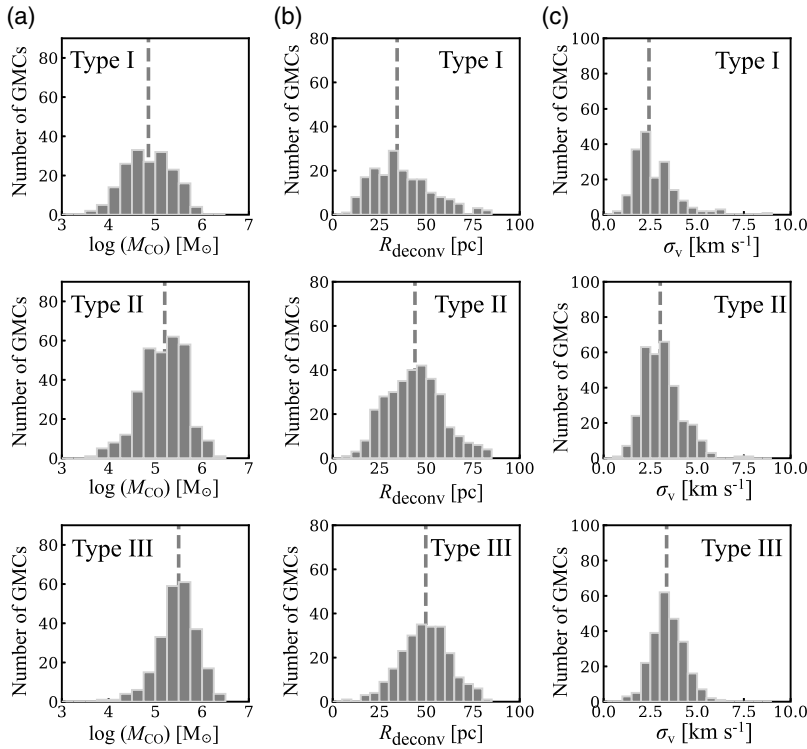
Figure 2. Frequency distributions of GMC properties, mass (a), radius (b), and velocity dispersion (c). The upper, middle, and lower panels indicate those of Type I, II, and III GMCs, respectively. Vertical dashed lines indicate the median for histograms.

3.3. *Basic properties of GMCs*

Figure 2 indicates histograms of mass, radius, and velocity dispersion for the three GMC types. The properties of Type I, II, and III GMCs are represented in the upper, middle, and lower panels, respectively. By comparing properties of GMCs, we found that the mass, size, and velocity dispersion slightly increase in the order of Type I, II, and III GMCs. Typical mass of Type II and III GMCs is larger than $10^5\,M_\odot$ while that of Type I GMCs is smaller than $10^5\,M_\odot$. This suggests that massive star-forming GMCs likely have their mass of $> 10^5\,M_\odot$. The GMCs are considered to form and evolve by continuous mass-accretion from local surrounding H I gas (e.g., Hennebelle & Pérault 1999; Koyama & Inutsuka 2000, 2002; Vázquez-Semadeni et al. 2007; Fukui et al. 2009; Inoue & Inutsuka 2012). In addition, cloud-cloud collisions can make a major contribution the mass growth ($\sim 10^6\,M_\odot$) and star formation in GMCs (e.g., Kondo et al. 2021; Tokuda et al. 2020; Muraoka et al. 2020).
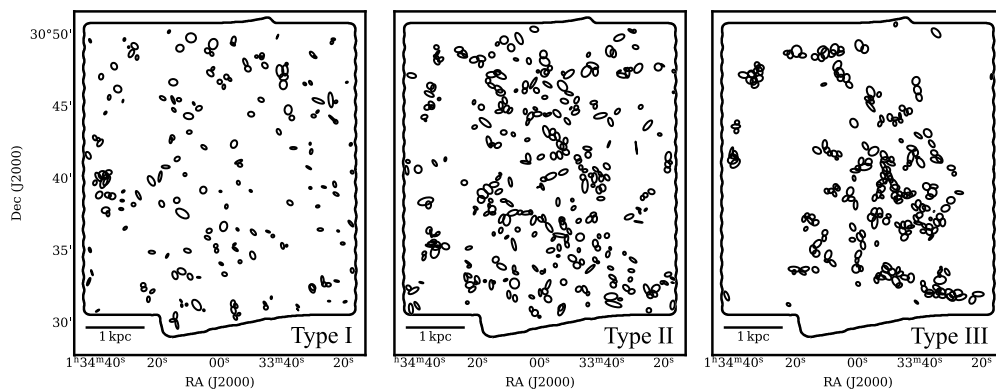
Figure 3. Distribution of GMCs in each type.

3.4. *Lifetime of GMCs in M33 based on the previous studies in LMC*

We estimate the GMC lifetime in M33 with reference to the previous studies of GMC evolution in LMC (Kawamura et al. 2009). First, the timescale for Type II GMC of 13 Myr was originally determined in LMC, and we assume that Type II GMC in M33 has the same timescale as the LMC. This is because Type II GMCs are considered to be less sensitive to the detection limit than Type I GMCs whose typical mass ($< \sim 10^5\,M_\odot$) is lowest in three types, and also less affected by gas dissipation due to stellar feedback than Type III GMCs which shows most active star formation. If we assume time-steady star formation rate in M33, the timescale of each type GMC is proportional to the number of them. From the number of Type I, II, III GMCs are 182 ($\sim 25\,\%$), 316 ($\sim 43\,\%$), and 238 ($\sim 32\,\%$), we estimated the timescale of Type I, II, and III GMCs to be 7 Myr, 13 Myr, and 10 Myr, respectively. The total lifetime of a GMC is estimated to 30 Myr in M33.

3.5. *The comparison of spatial distribution between GMCs and spiral arm*

Recent observations of GMCs in Local Group and nearby galaxies suggested that galactic scale events such as spiral shock and tidal interaction of galaxies play an important role in the massive star formation (e.g., Fukui et al. 2017; Tsuge et al. 2019; Tokuda et al. 2020; Muraoka et al. 2020). We investigated the spatial distribution of GMCs in each type and the relationships between the evolution of GMCs and galactic dynamics. Figure 3 shows the significant difference in the randomness of GMC distributions according to their types. Type I GMCs randomly distributed while Type III GMCs have a distribution like spiral arm. Then, we compared the distribution between GMCs and stellar spiral arms. M33 is a flocculent spiral galaxy, thus its spiral arms are less prominent. In order to clarify nonaxisymmetric structures such as the spiral arm, we created an axisymmetric model disk of M33 from the IRAC 3.6 μm data (Dale et al. 2009), and subtracted it from the original 3.6 μm image to form the residual image (Regan & Vogel 1994, Figure 4 a). The spiral arm structures are clearly seen. Figure 4 (b) shows the comparison between the 3.6 μm residual image and the distribution of type III GMCs. Most of Type III are distributed along the arms. We also found Type I GMCs are mainly distributed in the inter-arm and Type II GMCs are distributed not only in the arm but also in the inter-arm. These results suggest that GMCs tend to gradually evolve and move from both sides (leading and trailing sides) towards the arms, and the spiral arm plays an important role in massive star formation even in flocculent spiral galaxy M33.
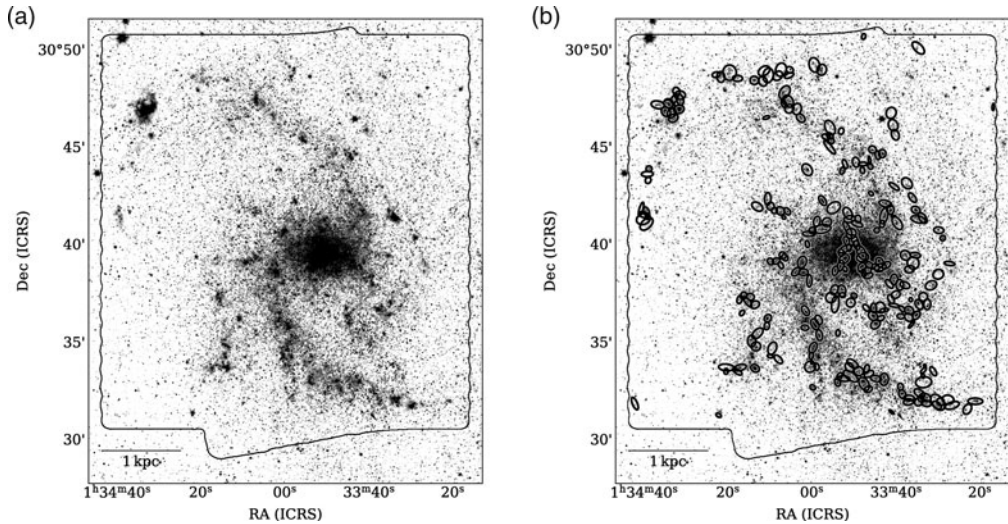
Figure 4. (a) Model-subtracted IRAC 3.6 μm image of M33. The spiral arm structures are clearly seen. The solid line shows the ACA observed area. (b) Distribution of Type III GMCs on (a). The ellipses represent Type III GMCs.

4. Summary

We conducted CO($J = 2$–1) survey in the nearest spiral galaxy M33 by ACA 7 m array and analyzed the combined ACA 7 m and IRAM 30 m ^{12}CO data with spatial resolution of ∼39 pc. We detected 736 GMCs and classified them into three types based on the association with H II regions and Hα luminosities. Properties of GMCs, the mass, size, and velocity dispersion slightly increase in the order of Type I, II, and III GMCs. Type I GMCs are mainly distributed in the inter-arm and Type II GMCs are distributed not only in the arm but also in the inter-arm. Type III GMCs are mostly distributed along the arms. This suggests that the spiral arm plays an important role in massive star formation. If we assume that the timescale of Type II GMCs in M33 is 13 Myr as in LMC, the timescales of Type I, II, III GMCs in M33 are estimated to be 7 My, 13 Myr, and 10 Myr, respectively. These timescales yield a GMC lifetime of 30 Myr.

References

Cornwell, T.,J. 2018, IEEE Journal of Selected Topics in Signal Processing, 2, 793
Corbelli, E., Braine, J., Bandiera, R., et al. 2017, *A&A*, 601, A146
Dale D. A., Cohen, S. A., Johnson, L. C. et al., 2009, *ApJ*, 703, 1
Druard, C., Braine, J., Schuster, K. F. et al., 2009, *A&A*, 567, A118,
Freedman, W. L., Madore, B. F., Gibson, B. K., et al. 2001, *ApJ*, 553, 47
Fukui, Y., Mizuno, N., Yamaguchi, R., et al. 1999, *PASJ*, 51, 745
Fukui, Y., Kawamura, A., Wong, T., et al. 2009, *ApJ*, 705, 1
Fukui, Y., Tsuge, K., Sano, H., et al. 2017, *PASJ*, 69, 3
Gratier, P., Braine, J., Rodriguez-Fernandez, N. J., et al. 2012, *A&A*, 542, A108.
Hennebelle, P. & Pérault, M. 1999, *A&A*, 351, 309
Hoopes, C. G. & Walterbos, R. A. M. 2000, *ApJ*, 541, 597
Hoopes, C. G., Walterbos, R. A. M., & Bothun, G. D. 2001, *ApJ*, 559, 878
Inoue, T. & Inutsuka, S.-. ichiro. 2012, *ApJ*, 759, 35
Kawamura, A., Mizuno, Y., Minamidani, T., et al. 2009, *ApJS*, 184, 1
Koch, E. W., Rosolowsky, E. W., Lockman, F. J, et al. 2018, *MNRS*, 479, 2505
Kondo, H., Tokuda, K., Muraoka, K., et al. 2021, *ApJ*, 912, 66
Koyama, H. & Inutsuka, S.-I. 2000, *ApJ*, 532, 980

Koyama, H. & Inutsuka, S.-. ichiro. 2002, *ApJL*, 564, L97

McMullin, J. P., Waters, B., Schiebel, D., Young, W., & Golap, K. 2007, Astronomical Data Analysis Software and Systems XVI, 376, 127

Muraoka, K., Kondo, H., Tokuda, K., et al. 2020, *ApJ*, 903, 94

Muraoka, K., Konishi, A., Tokuda, K., et al. 2022, *ApJ*, submitted

Pan, H. A., Schinnerer, E., Hughes, A., et al. 2022, *ApJ*, 927, 1

Regan M. W. & Vogel S. N. 1994, *ApJ*, 434, 536

Rosolowsky, E. W., Pineda, J. E., Kauffmann, J., et al. 2008, *ApJ*, 679, 1338

Rosolowsky, E. W., Hughes, A., Leroy, A., et al. 2021, *MNRS*, 502, 1

Tokuda, K., Muraoka, K., Kondo, H., et al. 2020, *ApJ*, 896, 36

Tsuge, K., Sano, H., Tachihara, K., et al. 2019, *ApJ*, 871, 1

Schinnerer, E., Hughes, A., Leroy, A., et al. 2019, *ApJ*, 887, 49

Vázquez-Semadeni, E., Gómez, G. C., Jappsen, A. K., et al. 2007, *ApJ*, 657, 870

Yamaguchi, R., Mizuno, N., Mizuno, A., et al. 2001, *PASJ*, 53, 985